Vietnam Journal of Earth Sciences, 45(3), 303-325, https://doi.org/ 10.15625/2615-9783/18411

Vietnam Journal of Earth Sciences
https://vjs.ac.vn/index.php/jse

Geochemistry and zircon U-Pb geochronology of the Dak Krong plutonic rocks in the Kontum Massif (central Vietnam) and their petrogenetic implications

Nguyen Kim Hoang[1,2], Nong Thi Quynh Anh[1,2], Pham Minh[1,2], Pham Trung Hieu[1,2*], Nguyen Thanh Thao[3]

[1]*Faculty of Geology, University of Science, Ho Chi Minh City, Vietnam*
[2]*Vietnam National University, Ho Chi Minh City, Vietnam*
[3]*South Vietnam geological mapping division, Ho Chi Minh City, Vietnam*

Received 10 November 2022; Received in revised form 23 April 2023; Accepted 9 June 2023

ABSTRACT

Dak Krong plutonic rocks are found in the Kontum Massif along the N-S-oriented Po Ko River and mainly within the distributive area of the Ben Giang-Que Son granitic bodies. The Hai Van complex crosscuts the Dak-Krong rocks. They are predominantly composed of plagioclase (35-47%), quartz (29-30%), K-feldspar (20-28%), and minor biotite (3-4%). Geochemically, they are characterized by meta- to peraluminous and high-K affinities and straddle I- and S-type granite fields. Zircon U-Pb dating results yielded two main magmatic stages (ca. 258 Ma and ca. 245 Ma) spanning two phases of magmatism presumably accepted as being associated with the Paleo-Tethys Ocean evolution: latest subduction to syn-collisional phases. The Hf isotope data from zircon with εHf(t) ranging between -6.4 and -0.5 indicates a crustal signature. From the results of εHf(t) values along with zircon Hf model ages (TDM2) ranging from 1165-1497 Ma, it is presumable that the Dak Krong plutonic rocks are the product of the partial melting of Mesoproterozoic crustal materials with a negligible contribution of mantle materials. Together with other Permian-Triassic magmatic complexes throughout the Kontum Massif (e.g., Ben Giang-Que Son, Hai Van, and Van Canh complexes) and other plutonic further to the north along the Truong Son Belt and the Song Ma suture zone, the Dak Krong plutonic rocks represent magmatism generated by the amalgamation of Indochina and South China during the Late Permian-Early Triassic, referred to as Indosinian orogeny.

Keywords: Geochemistry, zircon U-Pb geochronology, Dak Krong granites, Indosinian orogeny.

1. Introduction

Permian-Triassic plutonic rocks in northern Vietnam have been widely attributed to magmatism connected with the closure of a Paleo-Tethys branch along the Song Ma Suture Zone (Hieu et al., 2017, 2015, 2020; Hoa et al., 2008; Liu et al., 2012; Nakano et al., 2013; Thanh et al., 2019). During the late Paleozoic time, geological formations in northern to central Vietnam experienced a long-lasting evolution of three main stages associated with the Paleo-Tethys evolution: subduction (290-250 Ma), the collision between the South China and Indochina Blocks (250-240 Ma), and post-collision (240-210 Ma) (Hieu et al., 2017, 2015; Hoa et al.,

*Corresponding author, Email: pthieu@hcmus.edu.vn

2008; Liu et al., 2012). The subduction direction has been widely discussed, with the main opinion favoring the southward dip of the South China Block beneath the Indochina Block (Faure et al., 2014, Hieu et al., 2017, 2015).

Toward the south of the Song Ma zone, Permian-Triassic magmatic activities have also been widely recorded along the Truong Son belt and throughout the Kontum Massif in recent studies (Hung et al., 2022; Pham et al., 2022). These magmatic activities, usually referred to as Indosinian magmatism, that took place extensively, imprinted the Ordovician magmatic-metamorphic complexes and caused deformation and weak metamorphism in the Kontum Massif (Tran et al., 2014; Usuki et al., 2009). As Permian-Triassic magmatism is one of the significant clues to deducing regional magmatic-tectonic evolution in the Indochina block and adjacent areas, previous and recent works have conducted investigations on the petrogenesis of igneous rocks mainly along the Song Ma and Truong Son Belt, and most recently extended southward to the Kontum Massif (Hung et al., 2022).

Permian-Triassic plutonic rocks from the Kontum Massif have been widely regarded as three main complexes: (1) the Ben Giang-Que Son complex representing the arc-related plutonism, (2) the Hai Van complex representing syn- to late collisional plutonism, and (3) the Van Canh complex reported to form during the Early Triassic and representing syn- to post-collisional plutonism. Based on geochemical characteristics and zircon U-Pb dating results, plutonic rocks regarded as the Ben Giang-Que Son and Hai Van complexes found in the Kontum Massif span wide age ranges, ca. 363-242 Ma for Ben Giang-Que Son granitoids (Bui et al., 2010; Sang, 2011), and 242-224 Ma for Hai Van granites (Hieu et al., 2015). Geochemical data and isotopic compositions show that the most recent work interpreted the 251-229 Ma plutonic in southern Kontum Massif (i.e., Van Canh complex) as S-type granites characterized by medium to high potassium content. They were suggested to be derived from the melting of Paleoproterozoic crustal rocks during the Early Triassic continental collision (Hung et al., 2022). Therefore, crystallization ages of plutonic rocks in the Kontum Massif display a wide range corresponding to complexity in geochemical affinities. Regarding petrogenesis and tectonic environments generating Permian-Triassic magmas, divergent opinions have yet to be solved: whether all >250 Ma granitoids were only associated with the arc-related regime and <250 Ma plutonic rocks with the syn-collisional regime or there might be interferences of different magmatic stages during the transitional phase from the arc- to collision-related regimes.

This study presents new data on the geochemical characteristics, zircon U-Pb ages, and zircon Hf isotope composition of Dak Krong plutonic rocks to contribute to available data on Permian-Triassic magmatism in central Vietnam. On a regional scale, this study further aims to reaffirm the far-field influence southward of the subduction and its consequential Indochina-South China amalgamation event along the Song Ma Suture zone (called Indosinian Orogeny).

2. Geological setting and petrography

2.1. Geological setting

Vietnam is located along the eastern margin of the Indochina Block, bordered to

the northeast by the South China Block and to the west by the Sibumasu Block (Metcalfe, 2017). From the north to the south of Vietnam, three main structural zones resulting from the amalgamation of tectonic plates/blocks have been recognized, including the Truong Son belt, the Kontum Massif, and the Da Lat zone (e.g., Hoa et al., 2008; Lepvrier et al., 2004). The Truong Son belt in the north is bounded by the Song Ma suture, where numerous Permian-Triassic plutonic bodies of chemically variable composition have been recorded (Faure et al., 2014; Hieu et al., 2017; Metcalfe, 2017, 2013; Thanh et al., 2019; Thanh et al., 2011). Toward the south of the Truong Son Belt, the Kontum Massif was built up on the Proterozoic basement and is separated from the Truong Son Belt by the Tam Ky - Phuoc Son suture, which has been considered to be a remnant of an Early Paleozoic oceanic basin (Faure et al., 2018; Tran et al., 2014). Three lithological units recognized in the Komtum massif are the Kham Duc, Ngoc Linh, and Kan Nack complexes, which are intruded by per-aluminous granite and mafic plutons (Faure et al., 2018). The Kham Duc complex includes the north part composed of metamorphic rocks of low- to medium-grade facies (e.g., metapelite, metagraywacke, quartz schist, scattered amphibolite) and the southern part partly experiencing an Early Paleozoic crustal melting event responsible for migmatites and anatectic granites (addressed as the Chu Lai migmatitic complex). The Ngoc Linh, located south of the Kham Duc complex, is formed by metatexite and granitoid enclosing blocks of largely high-grade metamorphic rocks. The Kan Nack complex is recorded mainly to the southern part of the Kontum massif and formed by migmatites with (ultra) high temperature (U)HT granulite, charnockites, and enderbites. Migmatites and anatectic granites resulted from migmatization that occurred predominantly in the Ngoc Linh and Kan Nack complexes (interpreted as parts of a metamorphic core complex). The Dak Krong granites are mainly found within the distributive area of the Ngoc Linh complex.

Further to the south, the Dalat zone has been described as a continental magmatic arc resulting from the subduction of the Paleo-Pacific Ocean beneath the Indochina Block during the Late Mesozoic (Nguyen et al., 2004; Shellnutt et al., 2013; Thuy et al., 2004). The boundary between the Kontum Massif and the Dalat zone has not been drawn in previous works, and the Dalat zone appears to attach to the south of the Kontum Massif (Bao, 2000; Tri and Khuc, 2009).

As being located in the southern part of the Truong Son Belt, the Kontum Massif has been influenced by the tectonic activities which extensively took place along the Song Ma Suture zone and extended southward to the Truong Son Belt (Hieu et al., 2017, 2015; Hoa et al., 2008; Liu et al., 2012; Pham et al., 2022). The multi-phase and long-lasting tectonism along the suture zone generated mainly Permian to Triassic plutonism represented by three main complexes, namely Ben Giang-Que Son, Hai Van, and Van Canh respectively corresponding to subduction-related, syn- to late collisional, and post-collisional stages (Hieu et al., 2015; Hung et al., 2022; Liu et al., 2012; Sang, 2011).

Along with the northward Song Ma Suture Zone influence, the Kontum Massif presents numerous northwest-southeast left-lateral faults (Lepvrier et al., 2008, 2004). Additionally, it exposes ancient formations of generally high-grade metamorphic rocks of the Precambrian age in southern Kontum and the lower-grade Early Paleozoic sedimentary

rocks in the north. Triassic migmatites (Ngoc Linh and Kan Nack complexes) are evident in the high-grade metamorphic rocks in the southern Kontum Massif (Faure et al., 2018). The Song Bung Formation, which represents Anisian volcanogenic sediments belonging to the Nong Son Basin (Khuc, 2000), is a lens-shaped outcrop southeast of the sampling route (Fig. 1b).

Granites in the Dak Krong area display cataclastic-mylonitic structures and have mainly been attributed to the Ben Giang-Que Son Complex. They display a significant extent and distribution trend following the meridian direction along the Po Ko River (Fig. 1). Toward the northwest of the study area, the Hai Van Complex is exposed to a lesser extent. The Dak Krong granites are highly weathered and form a thick weathering rind up to tens of meters. The fresh bedrock is exposed only sporadically along the streams in the study area (Fig. 2).

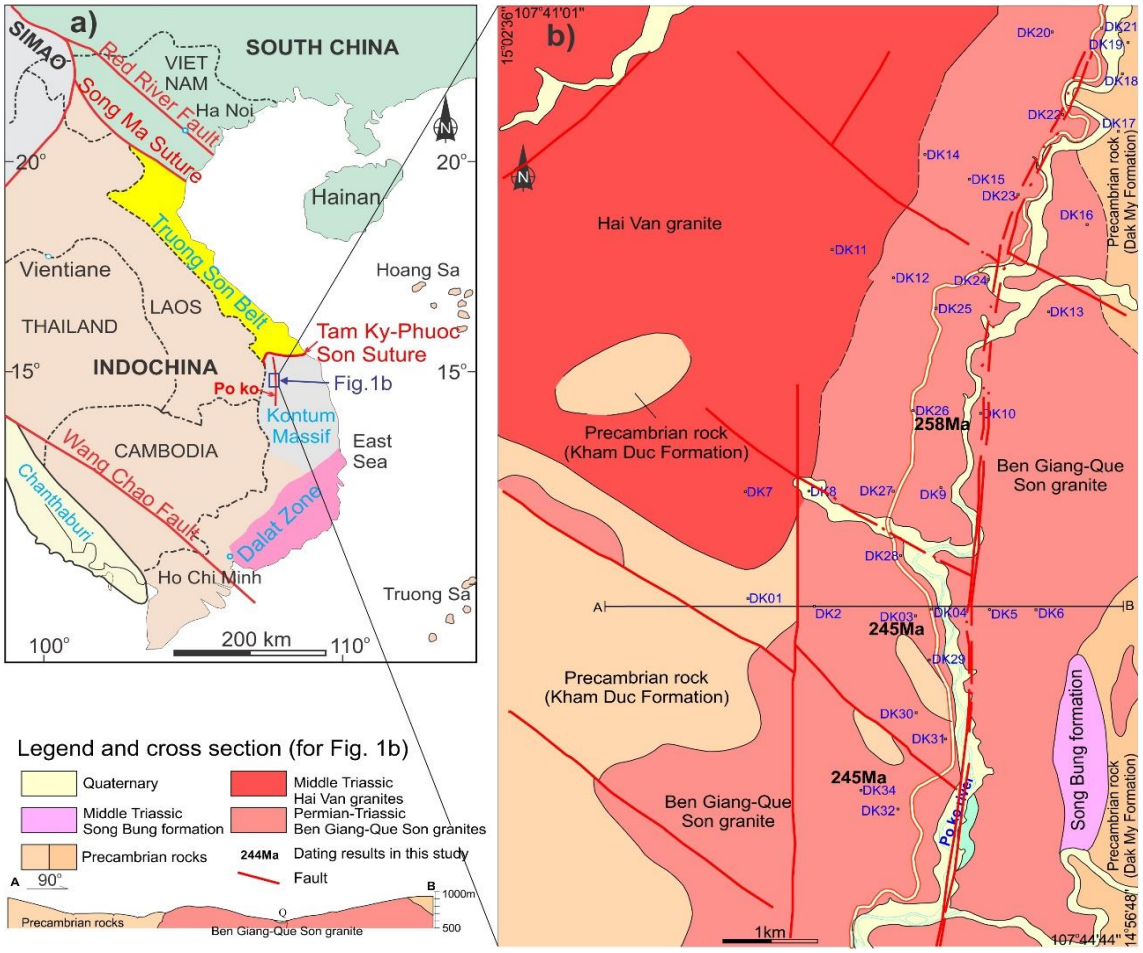

Figure 1. Schematic map showing the location and lithological components of the Dak Krong area (modified after Pham et al., 2022 and Trang, 1986)

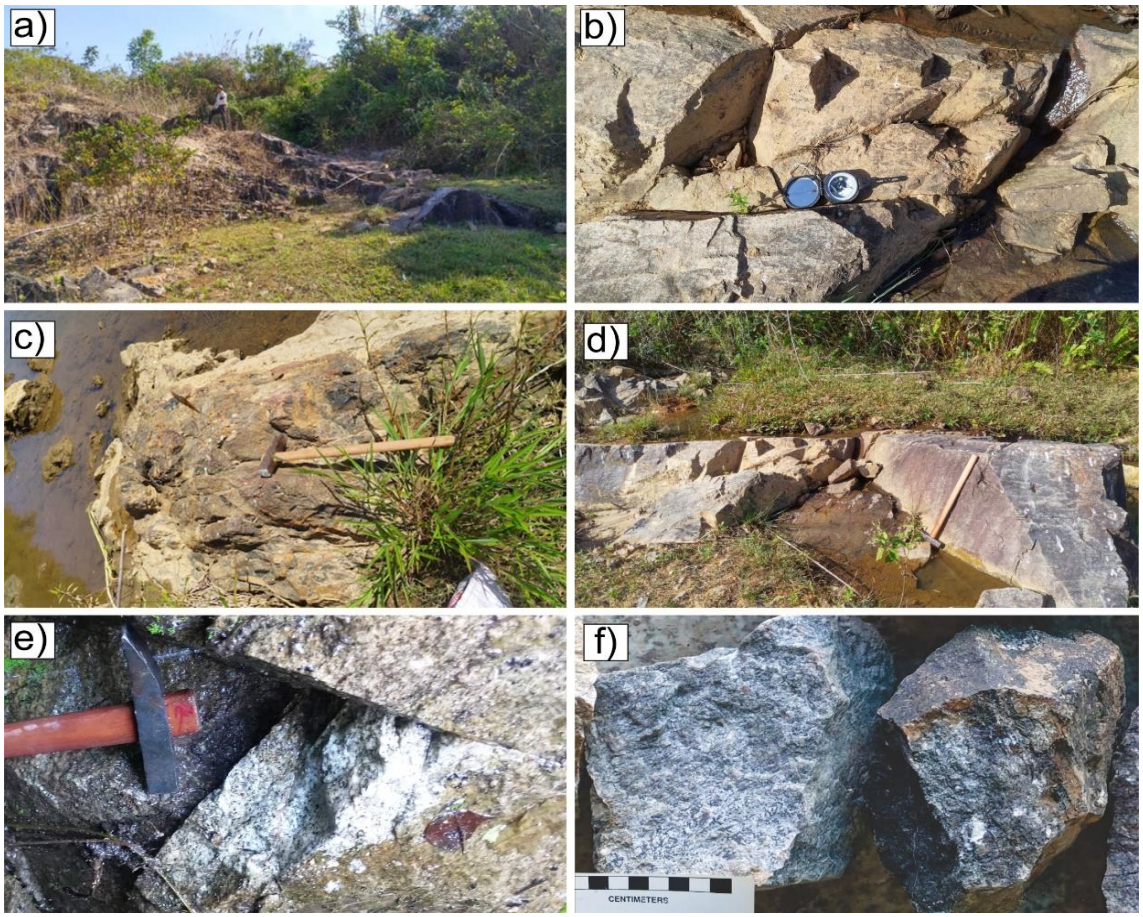

Figure 2. Outcrop features of the Dak Krong granites: a) Granodiorite of the Ben Giang-Que Son Complex where sample DK03 was collected; b) Granites exposed along the stream (DK03); c) Schist of the Kham Duc Complex found along the Po Ko River (DK24); d) Fine-grained granodiorite (phase 2); e) and f) Specimen samples of the Dak Krong granites

2.2. Petrography

Dak Krong plutonic rocks have been petrographically attributed to granites of the Ben Giang-Que Son complex in the Mapping scaled at 1:200.000 (Trang, 1986). They comprise two main phases: Phase 1 is composed of gabbrodiorite, hornblende-bearing diorite, and quartz diorite. Phase 2 is composed of cataclaszed pinkish-gray granite with variable grain size. The rocks of phase 2 are drastically altered and show cataclastic to mylonitic structure and strongly foliated and gneissic structure.

Granites of phase 1 are found as enclaved bodies in granites of phase 2, which penetrate and cause contact metamorphism to the metamorphic Kham Duc, and Dak My complexes (Fig. 1). A portion of the Kham Duc Complex is occasionally found in the Dak Krong granites as elongated enclaves.

The studied granites are covered by the Song Bung sedimentary formation and are crosscut by two-mica medium- to coarse-grained S-type granites of the Hai Van Complex. The regional meridian-oriented Po Ko River coinciding with the main fault is west-dipping and meridionally extends along the Dak Krong granite body. An accessory

NW-SE fracture and fault system also interrupt the studied granites. The survey route for sampling and field-working was implemented mainly along the Po Ko River, and studied samples were collected within phase 2 of Dak Krong granites.

Average mineral composition (in vol %) consists of plagioclase (35-47%), quartz (29-30%), K-feldspar (20-28%), minor biotite (3-4%), and hornblende. The common accessory minerals are zircon and ore minerals 1%. The secondary minerals found in most of the samples are kaolinite, sericite, limonite, chlorite, and calcite. Minerals were identified and investigated under the polarized-light microscope. A mineral assemblage of plagioclase + quartz + K-feldspar + biotite can be identified as follows (Fig. 3):

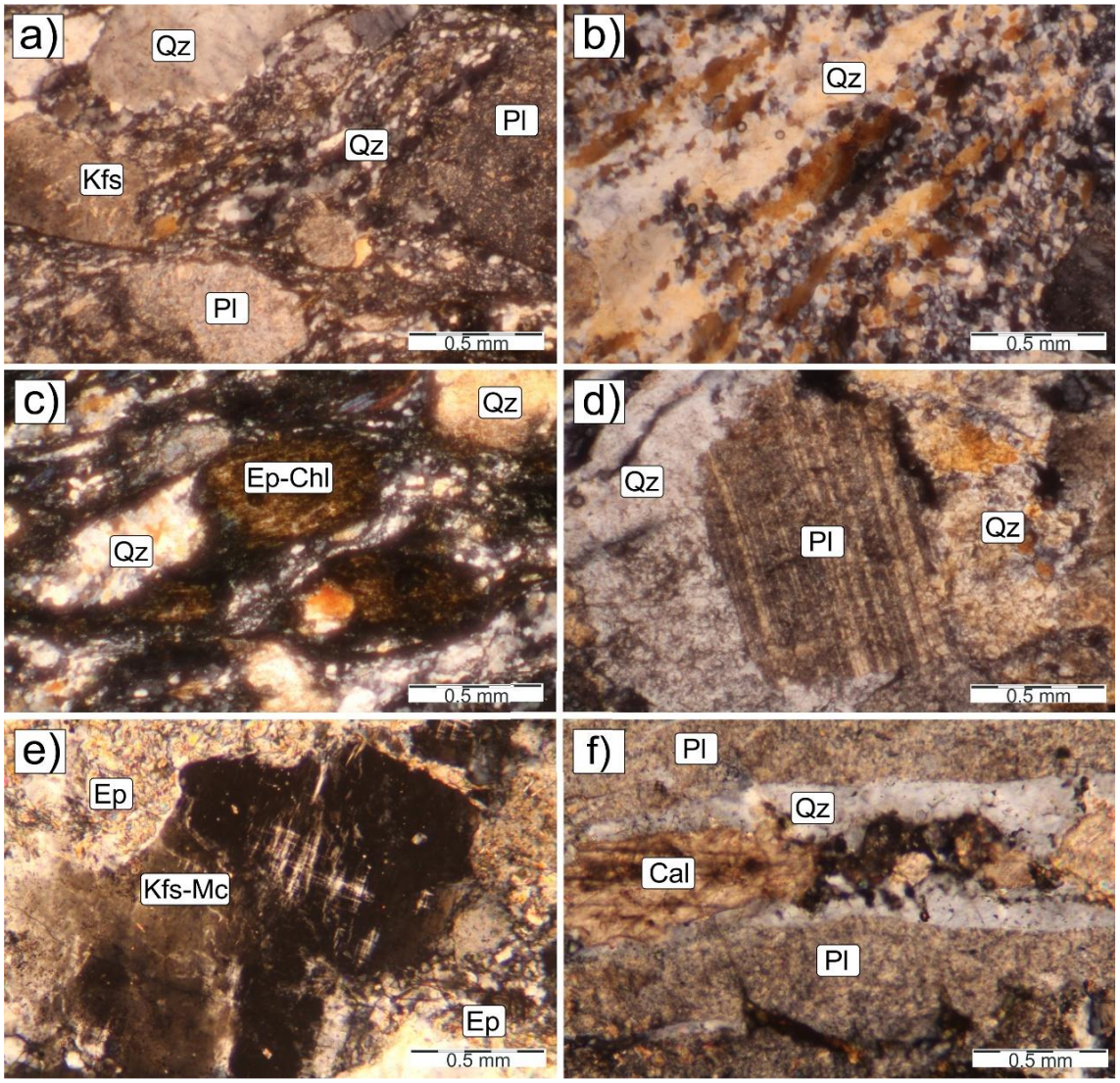

Figure 3. Cross-polarized light photomicrographs of the Dak Krong granites. Abbreviations of mineral names: Pl - plagioclase, Qz - quartz, Kfs - K-feldspar, Kfs-Mc - microcline, Ep - epidote, Chl - chlorite, Cal - calcite

Plagioclase with two groups (generations) can be recognized. Plagioclase of the main groups is tabular euhedral in shape, showing a common size of 0.5 × 1.2 mm and pronounced albite twinning and carlsbad and a zoning structure. The alteration, mainly sericitization, extensively occurs and obscures the optical appearance of plagioclase. Plagioclase can be categorized as andesine based on its optical appearance. Plagioclase of group 2 is mainly fine-grained (~0.05 mm) aggregated with K-feldspar of group 2 and quartz in deformed and foliated bands that surround and are disseminated in the plagioclase of group 1.

Quartz can be categorized into three groups. It is mainly present as single anhedral fine grains (~0.05-0.1 mm) or aggregated with K-feldspar and plagioclase of group 2 (fine grains) as weekly foliated bands penetrating or surrounding quartz of group 1. A small amount of quartz is anhedral, deformed, and corroded by K-feldspar and assemblages of deformed bands with a common size range of 0.4×0.6 mm, showing common micro fractures and typical undulose extinction. A few grains of quartz are present in micro veins of 0.2-0.5 mm in width penetrating K-feldspar and quartz of group 1.

K-feldspar can be categorized into two groups: Orthorclase is tabular, equant, and anhedral with a size range from 0.5×1.2 to 0.7×3.0 mm. Orthoclase shows typical carlsbad twinning and perthitic texture. It is commonly replaced by microcline. The most common secondary phase of orthoclase is kaolinite. Orthoclase is also present as fine grains aggregated with fine-grained plagioclase and quartz in micro veins.

Biotite is present as relic scales disseminated or aggregated and strongly chloritized with associated ore minerals and limonite.

Zircon, apatite, allanite, and ore minerals are the most common accessory phases. They are euhedral and prismatic. Allanite is brownish and shows a zoning structure. Secondary minerals such as calcite, sericite, and epidote can be observed as micro veins or aggregates that partially replace the primary minerals.

3. Analytical methods

Seven samples collected from the Dak Krong area were prepared for whole-rock chemical analyses. The measurement was conducted at the State Key Laboratory of Geological Process and Mineral Resources, China University of Geosciences, in Wuhan. Samples were powdered to a grain size of < 200 μm. Major element compositions were obtained using the XRF method (X-ray fluorescence spectrometry). The loss on ignition (LOI) was determined by heating 1 g of sample powder to 1000°C for 1 h. Minor and trace elements were obtained using Agilent 7500ce ICP-MS (inductively coupled plasma mass spectrometry) on dissolved samples. Fifty milligrams of each powdered sample were dissolved in the mixture of HF and HNO_3 at 190°C for 48 h in Teflon bombs for analyses. Reference sample GBW07103 was used for external quality control. Samples BHVO-2 and AGV-2 were used to verify the analytical accuracy. The analytical uncertainties are less than 5% for major and trace elements. The analytical procedure is presented by Hieu et al. (2015).

Three representative samples (DK03, DK26, and DK34) were selected for zircon LA-ICPMS analyses. Zircon samples were separated using a density technique and magnetic separator and randomly hand-picked under a binocular microscope. Zircon grains were mounted on epoxy resin and polished to

expose the inner parts of the grains for better cathodoluminescence images and age dating. Zircon U-Pb dating from three selected samples was conducted using a laser ablation inductively coupled plasma mass spectrometer (LA-ICP-MS) at the China University of Geosciences in Wuhan. A laser spot size of 32 μm and repetition of 6 Hz was applied for all analyses. Concordia diagrams and weighted mean ages were calculated and plotted using Isoplot/Excel (Ludwig, 2008). The results were reported with 2σ errors.

Hf isotopic analysis was obtained from the same zircon grains for U-Pb data. Zircon 91500 was used as a reference standard. The isotope compositions are presented in Table 3. The decay constant used to calculate the age is λ = 1.865×10-11year-1 (Scherer et al., 2001). The εHf(t) calculation was based on the crystallization age of zircon (t) and the measured ($^{176}Lu/^{177}Hf$) and ($^{176}Hf/^{177}Hf$) values. The present-day chondritic values $^{176}Lu/^{177}Hf$ = 0.0336 and $^{176}Hf/^{177}Hf$ = 0.282785 (Bouvier et al., 2008) and the depleted mantle values $(^{176}Hf/^{177}Hf)_{DM}$ = 0.28325 and $(^{176}Lu/^{177}Hf)_{DM}$ = 0.0384 (Griffin et al., 2000) were applied for calculations. The model ages of the T_{DM} mantle and the crustal substrate T_{DM2} (two-stage model) were calculated based on the isotope initial zircon $^{176}Hf/^{177}Hf$ ratios and U-Pb ages. The analytical results are shown in Table 4.

4. Analytical results

4.1. Whole-rock chemistry

The results of 07 samples for analysis of major and trace elements are presented in Table 1 and Table 2, respectively.

Table 1. Major element contents of the Dak Krong plutonic rocks

Sample	DK03	DK04	DK21	DK26	DK26/2	DK31	DK34
SiO_2	69.44	70.27	68.47	66.67	72.15	69.80	70.77
TiO_2	0.28	0.33	0.28	0.34	0.13	0.39	0.33
Al_2O_3	14.23	13.12	13.54	13.76	12.72	14.65	15.19
FeO	1.60	1.66	1.76	1.99	1.00	2.42	1.59
Fe_2O_3	0.18	0.19	0.20	0.22	0.11	0.27	0.18
$Fe_2O_3^t$	1.78	1.85	1.95	2.21	1.11	2.69	1.77
MnO	0.04	0.04	0.03	0.04	0.01	0.03	0.04
MgO	1.72	1.82	1.63	1.86	1.11	2.05	1.85
CaO	2.02	1.79	3.46	3.04	1.78	1.19	1.02
Na_2O	3.88	3.82	3.79	3.85	3.61	3.40	4.00
K_2O	4.06	4.03	4.85	4.15	4.36	4.70	4.97
P_2O_5	0.07	0.07	0.07	0.09	0.03	0.11	0.06
LOI	2.50	2.86	1.94	4.01	3.02	1.12	0.23
Total	101.8	101.85	101.97	102.23	101.14	102.82	102
A/CNK	0.98	0.94	0.76	0.84	0.92	1.14	1.10
A/NK	1.32	1.23	1.18	1.27	1.19	1.37	1.27
Fe^*	0.48	0.48	0.52	0.52	0.48	0.54	0.46
$Mg^\#$	65.76	66.05	62.34	62.46	66.29	60.22	67.44
T_{Zr}.Sat.C*	795.4	730.9	756.8	756.1	718.6	796.8	762.6
T_{Zr}.Sat.C**	745.8	670.9	687.3	691.6	657.1	754.0	712.5

A/CNK value: molar $Al_2O_3/(CaO + Na_2O + K_2O)$; A/NK value: molar $Al_2O_3/(Na_2O + K_2O)$ TZr.Sat.C* and TZr.Sat.C**: Temperature estimated using zircon saturation thermometers (Celsius) after Watson and Harrison (1983) and Boehnke et al. (2013), respectively

Table 2. Trace element contents of the Dak Krong plutonic rocks

Sample	DK03	DK04	DK21	DK26	DK26/2	DK31	DK34
Sc	2.33	1.80	0.60	2.13	1.53	2.66	2.88
V	18.40	11.70	16.70	22.00	8.46	41.00	28.90
Cr	10.90	6.71	6.49	9.41	6.92	14.00	8.44
Co	2.25	1.99	1.49	2.40	1.28	5.26	3.57
Ni	3.60	2.18	1.64	2.84	1.59	3.21	3.03
Cu	7.72	4.30	4.97	5.03	2.89	9.31	7.42
Zn	29.6	28.2	16.7	29.7	3.6	43.4	52.9
Ga	15.4	11.8	14.7	16.4	15.5	19.1	18.8
Rb	123	112	110	90	156	143	122
Sr	252	181	468	520	284	378	286
Zr	201	96	194	165	81	172	121
Nb	14.70	6.07	1.41	5.89	8.35	5.47	9.25
Cs	3.01	1.73	2.47	2.89	2.07	3.83	2.95
Ba	831	713	1400	1100	484	1400	608
Hf	6.75	2.89	5.67	4.96	3.06	4.63	3.85
Ta	1.14	0.67	0.07	0.55	0.99	0.23	0.73
Pb	17.20	22.70	15.20	15.20	21.00	13.60	28.00
Th	9.83	8.20	8.87	8.03	17.00	11.80	12.00
U	3.44	3.26	1.69	3.39	19.80	1.27	3.89
La	23.2	25.5	25.3	21.1	15.2	42.2	26.2
Ce	38.6	43.9	42.1	37.9	28.5	73.0	44.3
Pr	4.59	5.19	4.52	4.54	3.22	8.21	6.19
Nd	16.1	18.1	14.1	16.5	11.2	26.7	22.4
Sm	2.59	2.94	1.66	2.95	2.10	3.43	3.62
Eu	0.73	0.86	0.71	0.99	0.46	1.15	0.82
Gd	2.19	2.45	1.52	2.60	1.93	3.01	2.93
Tb	0.29	0.31	0.13	0.38	0.33	0.31	0.37
Dy	1.41	1.46	0.49	2.09	1.97	1.24	1.72
Ho	0.27	0.27	0.09	0.40	0.39	0.24	0.31
Er	0.82	0.78	0.33	1.13	1.17	0.71	0.94
Tm	0.12	0.11	0.05	0.16	0.18	0.09	0.13
Yb	0.79	0.71	0.41	0.98	1.20	0.60	0.83
Lu	0.13	0.10	0.08	0.14	0.19	0.10	0.13
Y	8.18	7.77	2.71	11.20	11.30	6.54	9.23
Li	11.8	8.8	14.4	12.5	4.1	15.7	22.1
Be	3.22	1.52	1.72	2.27	2.68	2.31	2.54
Mo	0.15	0.09	0.12	0.14	0.11	0.13	0.22
Cd	0.16	0.08	0.14	0.14	0.06	0.14	0.09
Sn	3.02	1.83	0.75	2.60	2.63	3.06	2.88
Ge	0.48	0.50	0.45	0.56	0.32	0.84	0.64
W	0.69	0.28	1.45	0.73	0.15	1.17	1.17
Mn							
As	18.70	18.30	18.90	18.80	19.50	19.10	18.80
Bi	0.27	0.14	0.09	0.05	0.16	1.33	0.16
10000Ga/Al	2.04	1.70	2.05	2.25	2.30	2.46	2.34
M	1.54	1.58	2.03	1.85	1.58	1.34	1.39
T Zircon	795.77	731.29	757.19	756.47	718.86	797.25	763.00
Eu/Eu*	0.94	0.97	1.37	1.09	0.70	1.09	0.77
∑LREE	85.81	96.49	88.39	83.98	60.68	154.69	103.53
∑HREE	6.02	6.19	3.11	7.88	7.35	6.29	7.36
∑REE	91.83	102.67	91.50	91.86	68.03	160.98	110.88
(La/Yb)n	21.20	25.83	44.05	15.49	9.09	50.53	22.62
(Tb/Yb)n	1.67	1.96	1.46	1.79	1.25	2.34	2.03
(La/Nd)n	2.84	2.78	3.54	2.52	2.67	3.11	2.30
Ybn	4.62	4.16	2.42	5.75	7.06	3.52	4.89

Table 3. LA-ICP-MS zircon U-Pb analytical data of the Dak Krong granites in Kontum massif

Sample	Th/U	Isotopic ratios						Age (Ma)				
		$^{207}Pb/^{206}Pb$	1σ	$^{207}Pb/^{235}U$	1σ	$^{206}Pb/^{238}U$	1σ	$^{207}Pb/^{235}U$	1σ	$^{206}Pb/^{238}U$	1σ	Conc%
DK03												
1*	0.51	0.05481	0.00065	0.35412	0.01096	0.04649	0.00115	308	8	293	7	95
2*	0.73	0.05194	0.00047	0.26216	0.00338	0.03662	0.00048	236	3	232	3	98
3*	0.72	0.10734	0.01018	0.20946	0.01770	0.01415	0.00061	193	15	91	4	47
4	0.17	0.05127	0.00052	0.28016	0.00408	0.03961	0.00052	251	3	250	3	100
5*	0.81	0.05868	0.00060	0.28485	0.00467	0.03509	0.00042	254	4	222	3	87
6*	0.77	0.05444	0.00049	0.49404	0.00995	0.06574	0.00128	408	7	410	8	100
7*	0.78	0.05118	0.00047	0.26136	0.00427	0.03696	0.00054	236	3	234	3	99
8*	0.22	0.05945	0.00381	0.26124	0.01627	0.03187	0.00048	236	13	202	3	86
9*	0.60	0.05693	0.00062	0.27442	0.00388	0.03488	0.00039	246	3	221	2	90
10*	0.19	0.11112	0.00528	3.10746	0.30682	0.16806	0.01225	1435	76	1001	68	70
11	0.18	0.05188	0.00046	0.27248	0.00352	0.03806	0.00047	245	3	241	3	98
12	1.05	0.05349	0.00056	0.29077	0.00410	0.03942	0.00052	259	3	249	3	96
13	0.35	0.05341	0.00491	0.28741	0.02461	0.03903	0.00130	257	19	247	3	96
14	0.53	0.05761	0.00479	0.30542	0.02326	0.03845	0.00128	271	18	243	3	90
15	0.26	0.05187	0.00411	0.27573	0.01990	0.03855	0.00126	247	16	244	4	99
16	0.29	0.05577	0.00748	0.30247	0.03892	0.03933	0.00149	268	30	249	3	93
17	0.39	0.05071	0.00383	0.27162	0.01853	0.03885	0.00125	244	15	246	3	101
18	0.59	0.05500	0.00177	0.28848	0.00872	0.03804	0.00043	257	7	241	3	94
19	0.34	0.05277	0.00147	0.27805	0.00713	0.03821	0.00041	249	6	242	3	97
20	0.30	0.05215	0.00097	0.27802	0.00513	0.03866	0.00042	249	4	245	3	98
DK26												
1	0.53	0.05172	0.00050	0.29333	0.00371	0.04110	0.00046	261	3	260	3	100
2*	0.29	0.05100	0.00067	0.27891	0.00397	0.03973	0.00051	250	3	251	3	100
3	0.39	0.05149	0.00093	0.29084	0.00611	0.04116	0.00073	259	5	260	5	100
4*	0.37	0.05155	0.00064	0.31270	0.00838	0.04398	0.00107	276	6	277	7	100
5*	0.74	0.05154	0.00091	0.27193	0.00494	0.03838	0.00050	244	4	243	3	100
6*	0.48	0.05122	0.00057	0.25563	0.00377	0.03620	0.00044	231	3	229	3	99
7	0.23	0.05109	0.00069	0.28477	0.00529	0.04050	0.00064	254	4	256	4	101
8	0.51	0.05092	0.00071	0.28263	0.00501	0.04025	0.00047	253	4	254	3	100
9	0.69	0.05201	0.00080	0.30258	0.00554	0.04218	0.00042	268	4	266	3	99
10*	0.23	0.05078	0.00077	0.27190	0.00532	0.03890	0.00058	244	4	246	4	101
11*	0.77	0.05100	0.00079	0.27026	0.00523	0.03850	0.00053	243	4	244	3	100
12*	0.86	0.06744	0.00097	0.38573	0.01659	0.04148	0.00132	331	6	262	4	79
13	0.24	0.05821	0.00540	0.32966	0.02851	0.04108	0.00137	289	4	259	3	90
14	0.25	0.05333	0.00459	0.30109	0.02397	0.04095	0.00134	267	4	259	4	97
15	0.30	0.05386	0.00494	0.30022	0.02564	0.04043	0.00135	267	5	255	3	96
16	0.56	0.05127	0.00430	0.28971	0.02234	0.04098	0.00134	258	4	259	3	100
17	0.20	0.05162	0.00070	0.28579	0.01176	0.04016	0.00126	255	4	254	3	100
16	0.56	0.05127	0.00430	0.28971	0.02234	0.04098	0.00134	258	4	259	3	100
17	0.20	0.05162	0.00070	0.28579	0.01176	0.04016	0.00126	255	4	254	3	100
18	0.30	0.05285	0.00401	0.29533	0.02020	0.04053	0.00133	263	5	256	3	97
19	0.22	0.05313	0.00423	0.30321	0.02204	0.04139	0.00134	269	5	261	4	97
20*	0.29	0.05921	0.00130	0.32765	0.02130	0.04014	0.00135	288	5	254	3	88
21	0.30	0.05203	0.00375	0.29614	0.01909	0.04128	0.00133	263	5	261	4	99
22	0.31	0.05440	0.00095	0.30805	0.01605	0.04108	0.00132	273	5	260	4	95
23	0.37	0.05541	0.00106	0.31263	0.01782	0.04093	0.00135	276	5	259	3	94
24	0.14	0.05269	0.00063	0.29781	0.01095	0.04100	0.00129	265	5	259	3	98
DK34												
1	0.97	0.05124	0.00129	0.26339	0.00628	0.03754	0.00051	237	5	238	3	100
2	0.56	0.05080	0.00102	0.26527	0.00579	0.03802	0.00054	239	5	241	3	101
3	0.86	0.05172	0.00081	0.28740	0.00627	0.04030	0.00061	257	5	255	4	99
4*	0.62	0.06875	0.00346	0.36832	0.01390	0.03989	0.00046	318	10	252	3	79
5	0.82	0.05394	0.00262	0.28118	0.01322	0.03781	0.00045	252	10	239	3	95
6*	0.29	0.05720	0.00173	0.53036	0.01442	0.06725	0.00088	432	10	420	5	97
7*	0.86	0.06880	0.01008	0.36703	0.05357	0.03869	0.00052	317	40	245	3	77
8	1.22	0.05133	0.00094	0.27479	0.00653	0.03888	0.00070	247	5	246	4	100
9*	0.22	0.06368	0.00866	0.71429	0.08598	0.08135	0.00514	547	51	504	31	92
10	1.18	0.05134	0.00085	0.27113	0.00428	0.03842	0.00050	244	3	243	3	100
11	0.39	0.05138	0.00138	0.28207	0.00867	0.03898	0.00087	252	7	247	5	98
12	0.83	0.05249	0.00139	0.29145	0.00882	0.03966	0.00088	260	7	251	5	97
13	0.53	0.05189	0.00143	0.28068	0.00882	0.03890	0.00087	251	7	246	5	98
14	0.43	0.05252	0.00146	0.28984	0.00927	0.03922	0.00087	258	7	248	5	96
15	0.34	0.05248	0.00194	0.28275	0.01222	0.03883	0.00089	253	10	246	6	97
16	0.18	0.05119	0.00149	0.27133	0.00904	0.03848	0.00085	244	7	243	5	100
17	0.44	0.05484	0.00318	0.28150	0.01928	0.03791	0.00095	252	15	240	6	95
18	0.45	0.05268	0.00154	0.27045	0.00895	0.03822	0.00083	243	7	242	5	100
19	0.11	0.05580	0.00160	0.29543	0.00969	0.03845	0.00083	263	8	243	5	92
20	0.15	0.05364	0.00196	0.29687	0.01269	0.03884	0.00087	264	10	246	5	93

Note: * Dated spots excluded from weighted mean age calculation due to their low concordance or their deviation from the main age clusters

Table 4. Zircon Hf isotopic composition of the Dak Krong plutonic rocks

Sample	$^{176}Yb/^{177}Hf$	$^{176}Lu/^{177}Hf$	$^{176}Hf/^{177}Hf$	± 2σ	Age (Ma)	$\varepsilon_{Hf}(t)$	± 2σ	T_{DM1}(Ma)	T_{DM2}(Ma)
DK03									
DK03 - 1	0.046149	0.001040	0.282382	13	293	-7.6	0.7	1231	1600
DK03 - 2	0.078637	0.001677	0.282530	13	232	-3.7	0.7	1040	1338
DK03 - 3	0.041819	0.000887	0.282477	13	250	-5.1	0.7	1092	1428
DK03 - 4	0.079187	0.001560	0.282532	14	222	-3.8	0.7	1034	1337
DK03 - 5	0.045422	0.001094	0.282373	14	410	-5.4	0.7	1245	1572
DK03 - 6	0.124485	0.002609	0.282603	13	234	-1.2	0.7	959	1202
DK03 - 7	0.094345	0.002136	0.282590	19	221	-1.9	0.9	966	1229
DK03 - 8	0.091483	0.001983	0.282461	20	241	-6.0	0.9	1148	1473
DK03 - 9	0.073753	0.001564	0.282477	17	249	-5.2	0.8	1112	1435
DK26									
DK26 - 1	0.047468	0.001032	0.282499	12	251	-4.3	0.7	1066	1387
DK26 - 2	0.060710	0.001388	0.282543	13	260	-2.6	0.7	1014	1301
DK26 - 3	0.076200	0.001778	0.282443	14	277	-5.9	0.7	1168	1494
DK26 - 4	0.078727	0.001757	0.282477	14	229	-5.7	0.7	1118	1444
DK26 - 5	0.053399	0.001211	0.282463	12	256	-5.5	0.7	1122	1457
DK26 - 6	0.064874	0.001458	0.282519	13	254	-3.6	0.7	1049	1349
DK26 - 7	0.083513	0.001876	0.282510	14	266	-3.7	0.7	1074	1366
DK26 - 8	0.030079	0.000733	0.282498	13	246	-4.4	0.7	1059	1388
DK26 - 9	0.061541	0.001409	0.282446	14	244	-6.4	0.7	1152	1497
DK34									
DK34 - 1	0.064866	0.001405	0.282512	15	238	-4.2	0.7	1059	1370
DK34 - 2	0.093431	0.002100	0.282619	25	241	-0.5	1.0	923	1165
DK34 - 3	0.036723	0.000830	0.282493	13	255	-4.4	0.7	1068	1395
DK34 - 4	0.076653	0.001724	0.282458	13	252	-5.8	0.7	1144	1472
DK34 - 5	0.049671	0.001288	0.282613	12	421	3.3	0.7	911	1100
DK34 - 6	0.058715	0.001289	0.282501	16	246	-4.4	0.8	1070	1387
DK34 - 7	0.041682	0.000949	0.282501	12	243	-4.4	0.7	1060	1384

Dak Krong samples are plotted along with samples of coeval ages in the Kontum Massif in recent research (Hieu et al., 2015; Hoa et al., 2008; Hung et al., 2022; Pham et al., 2022; Shi et al., 2015) for comparison. Geochemical compositions show a medium to high SiO_2 content ranging between 66.67 and 72.15 wt%, Al_2O_3 from 12.72 to 15.19 wt%, and high total alkali (Na_2O+K_2O) ranging from 7.85 to 8.97 wt% (Fig. 4). Seven samples from Dak Krong plutonic rocks plotted on classification diagrams according to (Cox et al., 1979) based on SiO_2 and total alkali (Na_2O+K_2O) show concentrated petrographical compositions of the granite field (Fig. 4). They show a wide range of aluminum saturation index (ASI = 0.84-1.10) with most of them falling in the meta luminous field (Shand, 1943). Also, in Fig. 4, analyzed samples fall mainly into the high-K field (Peccerillo and Taylor, 1976) and the I-type granite fields, while a few samples point to the S-type granite field. The potassium content of the studied samples is dominant over sodium content, with a narrow range of low Na_2O/K_2O ratios (0.72-0.95) and K_2O ranging from 4.03 to 4.97. On the rock classification diagram after (Whalen et al., 1987), samples dominantly fall into the S- and I-type fields. The CIPW norm calculation results are relatively identical with petrographical compositions associated with plagioclase, quartz, K-feldspar, and minor hypersthene. The loss on ignition varies from 0.23 to 4.01 wt%.

Considering the ambiguity in S- and I-type affinities of the Dak Krong samples, they are compared with both I- and S-type granitoid samples from the Kontum Massif. The chemical compositions of the studied samples

especially well overlapped with samples of S-type granites (Hieu et al., 2015; Hung et al., 2022; Shi et al., 2015) and fractionated I-type granitoids (Shi et al., 2015) in Kontum with high and equivalent SiO_2 content to the studied rocks. Figure 5 shows the variation of major oxides with increasing SiO_2. Noticeably, the studied samples and granitoid samples from the Kontum Massif present a continuity in chemical variation trend, which may indicate that their fractionation is relatively continuous but at different degrees.

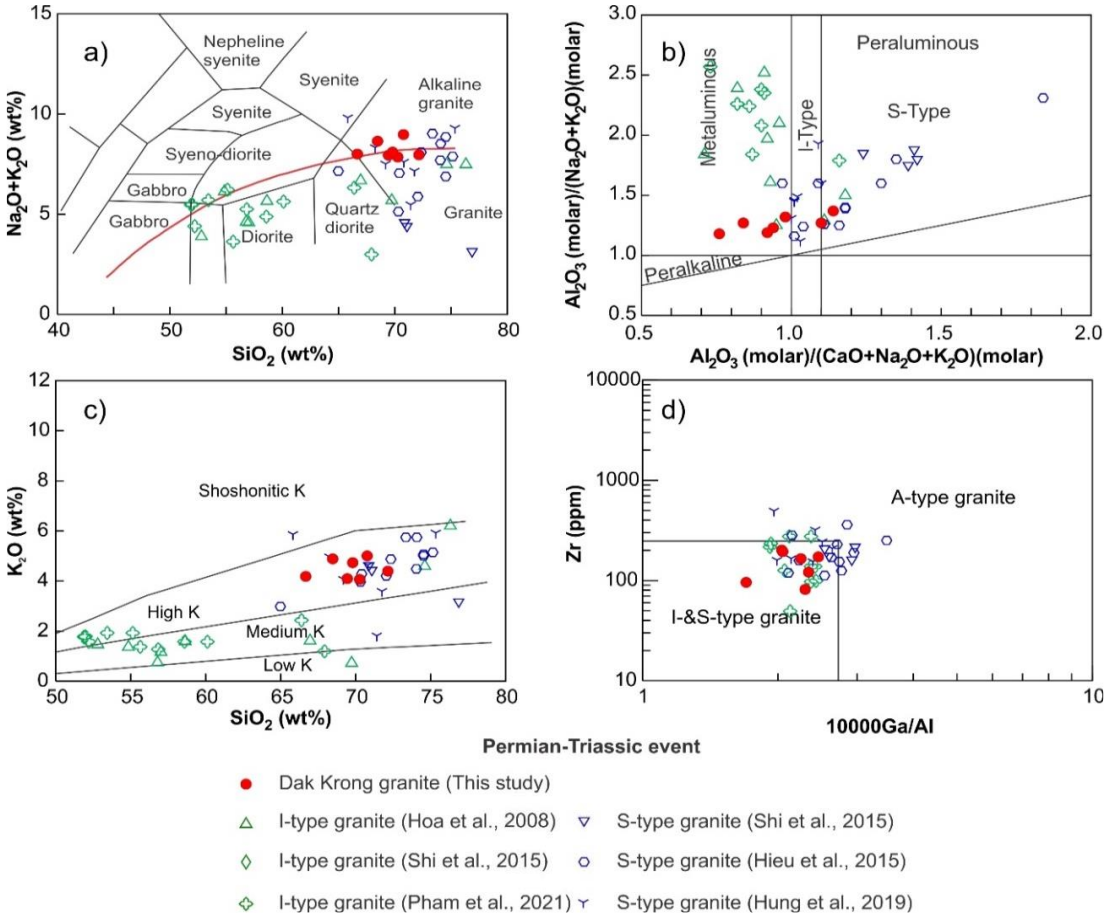

Figure 4. Classification diagrams of the Dak Krong granites: a) TAS diagram (Cox et al., 1979); b) A/CNK vs A/NK diagram (Shand, 1943); c) K_2O vs SiO_2 diagram defining magma series (Peccerillo and Taylor, 1976); and d) A-type and I- S-type granitoid discrimination (Whalen et al., 1987)

The total rare earth element concentration of the Dak Krong plutonic rocks ranges from 91.50 to 160.98 ppm. Generally, Dak Krong samples indicate the enrichment of light rare earth elements and depletion of heavy rare earth elements. A fractionated REE pattern is shown in the chondrite-normalized REE diagram with a variable anomaly of Eu (Eu/Eu* = 0.70-1.37) (Fig. 6). The pattern of one sample (DK21) deviates from the common trend with a significant depletion of HREEs possibly due to the fractionation of HREE- bearing minerals (e.g., garnet; Rollinson, 2014), which also cause this sample to lower the concentration of Nb, Ta, Yb, and Y in Fig. 7. The primitive mantle-normalized spider diagram after (Sun and McDonough, 1989) indicates enrichment in

Cs, Rb, Th, U, Pb, and Nd but depletion in Nb, Ta, P, Eu, and Ti (Fig. 6). The Eu and Ba contents without clearly negative or positive anomalies may indicate that the fractionation of plagioclase or K-feldspar is insignificant in the magma generating the studied rocks. According to the tectonic classification for granites (Harris et al., 1986; Pearce et al., 1984), collected samples are mainly plotted in the volcanic arc granite field, with two out of seven samples straddling the boundary between the volcanic arc granite and the syn-collision granite fields (Fig. 7). Zircon saturation temperature (Watson and Harrison, 1983) was estimated at a range of 719-797°C (Fig. 7). A more updated estimation of zircon saturation temperature conducted by Boehnke et al. (2013) shows a lower range of temperatures (657-754°C) for granites in Dak Krong.

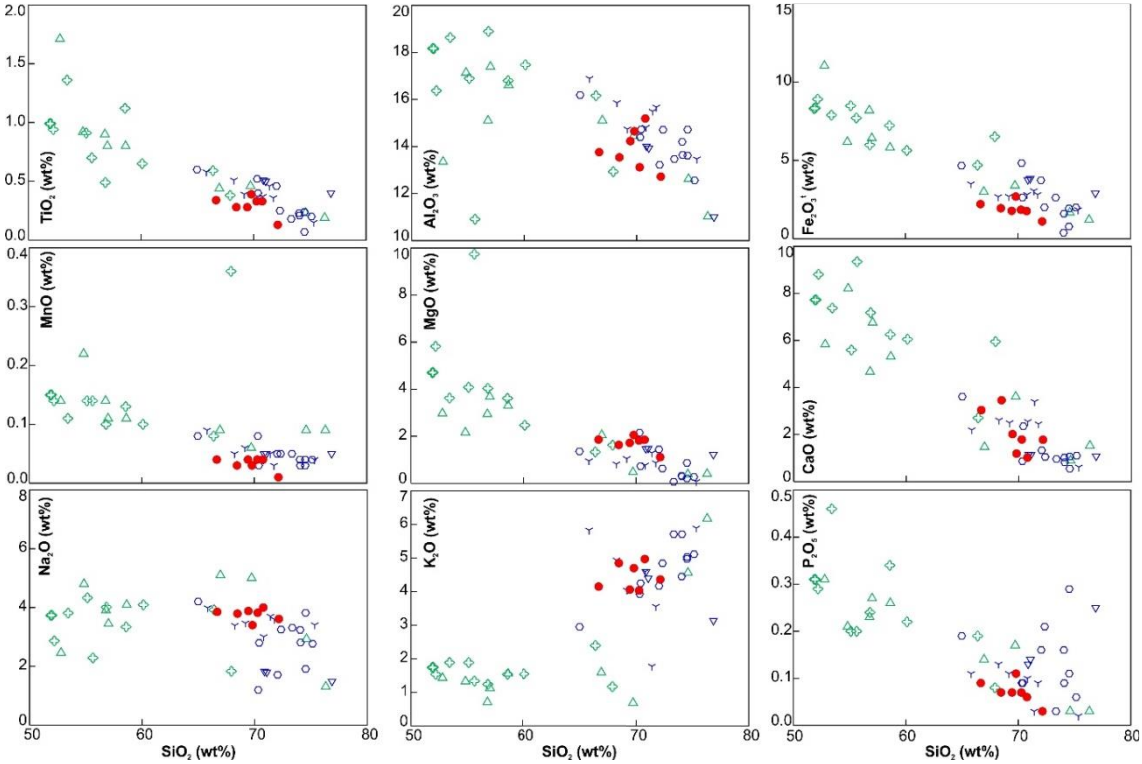

Figure 5. Harker diagrams of major oxides vs SiO_2 (see Fig. 4 for symbol explanation)

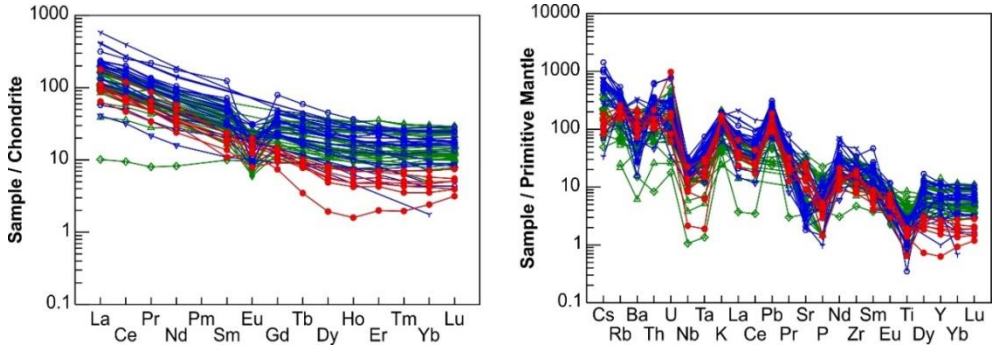

Figure 6. Chondrite-normalized and primitive mantle-normalized patterns for Dak Krong granites (see Fig. 4 for symbol explanation)

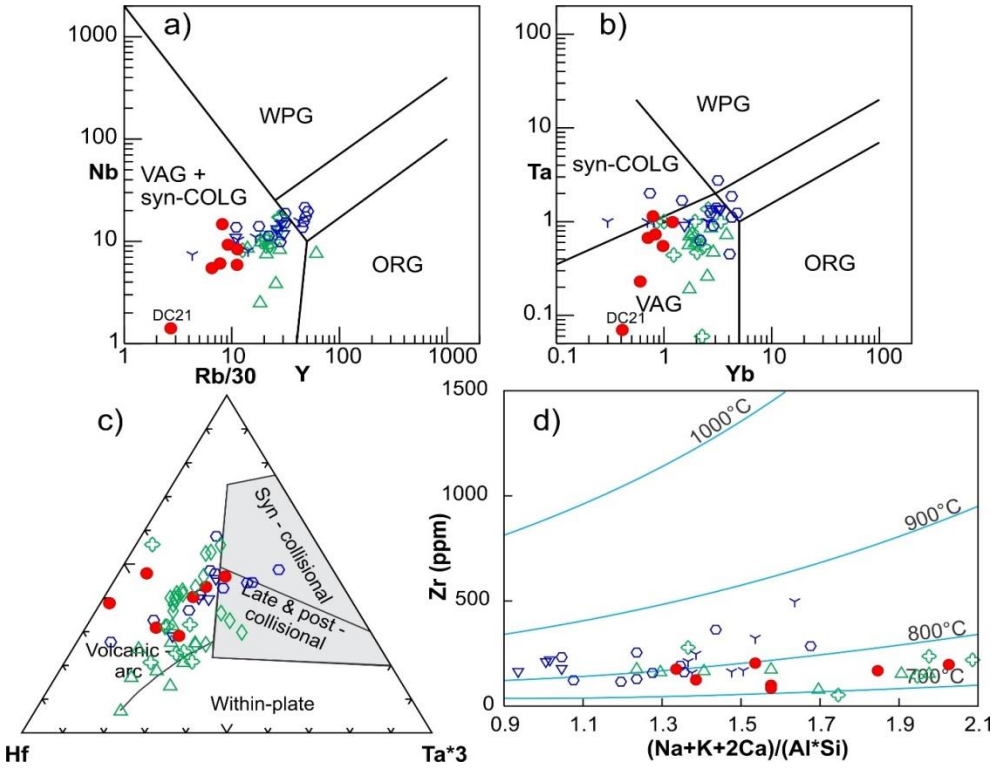

Figure 7. (a-c) Geotectonic discrimination (Pearce et al., 1984; Harris et al., 1986), (d) Estimated zircon saturation temperature of granites after Watson and Harrison (1984) (see Fig. 4 for symbol explanation)

4.2. Zircon U-Pb geochronology

In cathodoluminescence (CL) images, representative zircon grains from the studied samples of the Dak Krong granites are subhedral to euhedral and weakly transparent. They show light CL color in the cores and the transitional zone from core to rim, while the rims have dark aureoles. The grain size ranges from 100 to 250 μm in length and 50 to 100 μm in width. Their CL images show typical oscillatory zonation in most zircon inner zones and cores, indicating their magmatic origin.

Samples DK03, DK26, and DK34 were selected for age-dating analyses. 64 spots on 64 corresponding selected zircon grains are dated with LA-ICP-MS, and dating results are presented in Table 3. The Th/U ratios from analyzed spots with high values of 0.11-1.22 (> 0.1) indicate a magmatic origin of zircon (Hoskin and Schaltegger, 2003). The dating results are plotted on Wetherill concordia diagrams (Fig. 8). The weighted mean ages calculated for $^{206}Pb/^{238}U$ age values of concordant or nearly concordant spots show two age clusters: ca. 245 Ma and ca. 258 Ma. Several dated spots plotted below the concordia curve may indicate a lead loss.

Sample DK03: Twenty zircon grains from this sample were dated, of which eleven analyzed spots were concordant and nearly concordant. They yielded a zircon $^{206}Pb/^{238}U$ age range mainly from 241 to 250 Ma with a weighted mean $^{206}Pb/^{238}U$ age of 245.2± 2.2 Ma (MSWD = 1.19, n = 11) (Fig. 9a).

Sample DK26: Twenty-four zircon grains were dated, of which sixteen were concordant or nearly concordant. They yielded a zircon 206Pb/238U age range mainly from 254 to 266 Ma with a weighted mean 206Pb/238U age of 258.4 ± 1.6 Ma (MSWD = 0.97, n = 16) (Fig. 9b).

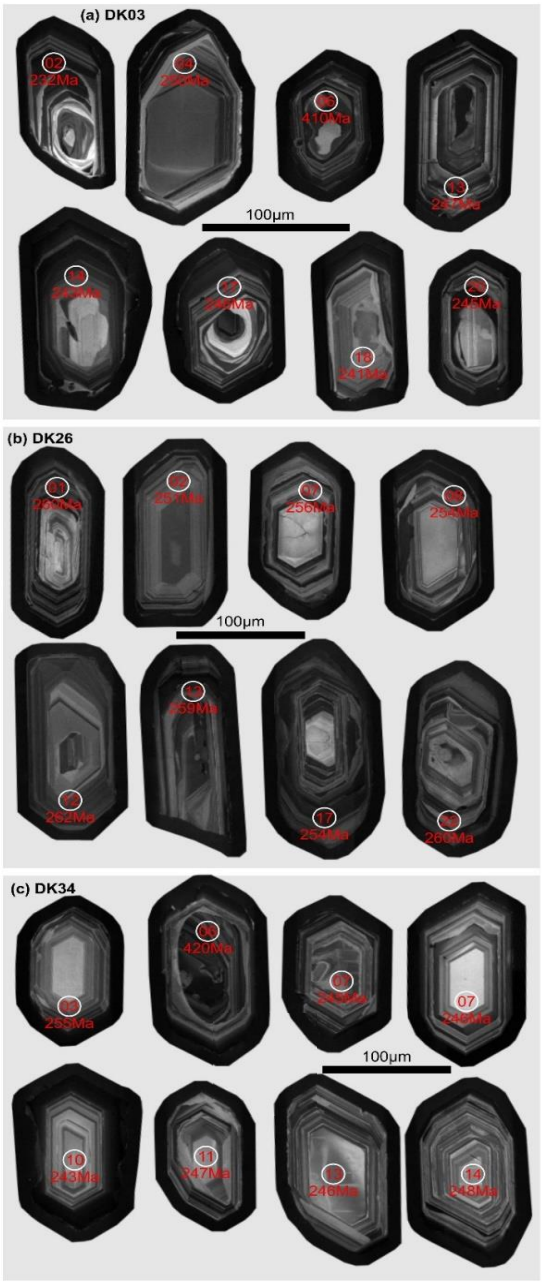

Figure 8. Cathodoluminescence (CL) images of representative zircon grains from the Dak Krong plutonic rocks

Sample DK34: Twenty zircon grains were dated, of which sixteen were concordant or nearly concordant. They yielded a zircon $^{206}Pb/^{238}U$ age range mainly from 238 to 255 Ma with a weighted mean age of $^{206}Pb/^{238}U$ age of 243.6 ± 2.5 Ma (MSWD = 1.3, n = 16) (Fig. 9c). Apart from the major age clusters of ca. 258 Ma and ca. 244 Ma, scattered old spots were dated at ~410 (sample DK03) and ~420 Ma (sample DK26) which might indicate xenocrystic dates of zircon.

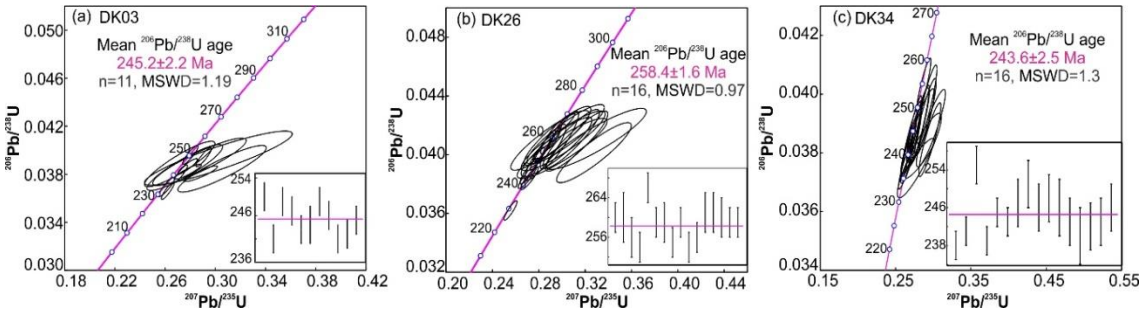

Figure 9. Zircon U-Pb concordia and weighted mean diagrams of the Dak Krong plutonic rocks

4.3. Hf isotopic composition

Zircon Lu-Hf isotope results from granitic samples DK03, DK26, and DK34 of the Dak Krong plutonic rocks are presented in Table 4 and Fig. 10.

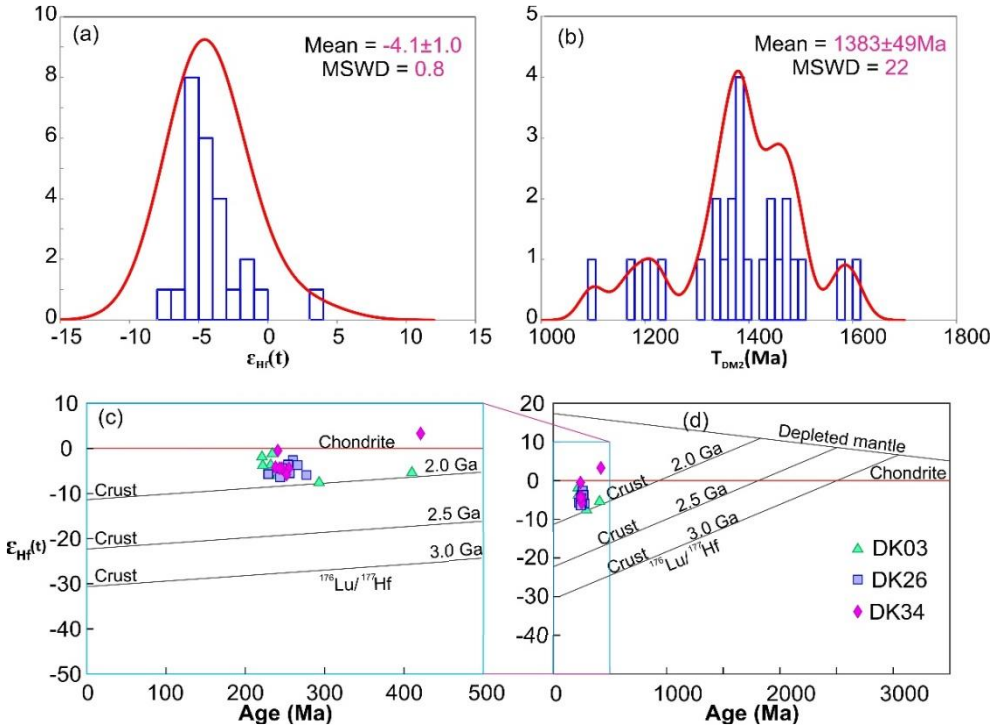

Figure 10. (a) and (b) Histograms of zircon εHf(t) values and Hf isotope model ages of the Dak Krong plutonic rocks; and (c) and (d) εHf(t) versus model ages diagram showing Hf depleted mantle model ages calculated for the Dak Krong samples

The εHf(t) was calculated based on the zircon U-Pb ages and mainly yielded values from -6 to -0.5 for magmatic zircons of the ca. 245 Ma group and a similar range from -6.4 to -2.6 for zircons of the ca. 258 Ma group. Scattered analyzed spots with old crystallization ages (e.g., ca. 420 Ma and ca. 410 Ma with εHf(t) value for 420 Ma spots recorded abnormally at +3.3) are excluded from data interpretation. The studied rocks define a narrow range of εHf(t), which falls slightly below the CHUR evolution line. The initial $^{176}Hf/^{177}Hf$ ratios of Dak Krong granites mainly range from 0.282373 to 0.282619,

slightly lower than the CHUR $^{176}Hf/^{177}Hf$ ratio. Their zircon Hf model ages (TDM2) range 1165-1497 Ma, corresponding to the Mesoproterozoic time.

5. Discussions

5.1. Emplacement age

Zircon U-Pb age dating results give two pronounced age ranges, ca. 258 Ma and ca. 245 Ma. Temporally, they respectively correspond to the subduction and syn-collisional stages of Paleo-Tethys evolution extensively recorded along the Song Ma Suture Zone and Truong Son Belt regarded as Indosinian Orogeny (e.g., Hieu et al., 2017, 2015, 2020; Hoa et al., 2008; Liu et al., 2012; Nakano et al., 2013; Thanh et al., 2019). However, we found scattered dated spots of the younger cluster, i.e., ca. 245 Ma in the age cluster of ca. 258 Ma and vice versa. This indicates a slight overlap of these two main magmatic stages. Therefore, different magmatic stages might have interferences during the transitional phase from the arc- to collision-related regimes.

The age dating results of the studied rocks relatively align with recent dating results on Permian-Triassic plutonic rocks throughout the southern Truong Son Belt and Kontum Massif, e.g., Cha Val plutonic (258-249 Ma, Pham et al. (2021) and Van Canh plutonic (251-229 Ma, Hung, et al., 2021). The dated age is coeval with the crustal melting event at around 250-240 Ma (Faure et al., 2018). That proposes a possible connection of the migmatization found in the Dak Krong samples with the second migmatic event in the Early Triassic recorded by Faure et al. (2018).

Considering the emplacement timing of Paleo-Tethys closure-related intrusive magmas along the Song Ma Suture zone, Truong Son Orogenic Belt, and recent records throughout the Kon Tum massif, the emplacement timing of Dak Krong granites span a wide range from the latest arc-related stage to syn-collisional stage. An explicit time correlation should not be made based only on dating results but also on geological field relationships. Accordingly, the zircon dating results are well identical to the field observations where Dak Krong granites are crosscut by the Hai Van complex (242-224 Ma; Hieu et al., 2015) and are covered by the Song Bung sedimentary formation (Middle Triassic age). Therefore, the emplacement age Dak Krong plutonic rocks can be presumably defined in Late Permian to Early Triassic age and coeval with the widespread Permian-Triassic magmatism recognized in the Song Ma Suture Zone and Truong Son Belt.

The scattered dated zircon spots with dates of 410 and 420 Ma might be an indicator of the Early Devonian magmatism, usually referred to as the Early Paleozoic orogenic magmatic activity and related to the Tam Ky-Phuoc Son and as mentioned above. However, due to the deficiency of the current dataset quantity, further studies are required before being able to draw a solid conclusion from this statement.

5.2. Petrogenesis

The Dak Krong granites are categorized as a meta- to peraluminous group with a high-K affinity. The petrographical signatures typical for S-type granites, such as ancient metasedimentary xenoliths or aluminum-rich minerals (e.g., muscovite and cordierite) have not been found. Although chemical composition does not pronouncedly show characteristics for S-type granites, the isotopic Lu-Hf compositions with εHf ranging between -6.4 and -0.5 indicate a crustal signature of the Dak Krong granites. The Hf model ages of ca. 1.2-1.4 Ga suggest that the Dak Krong plutonic rocks were derived from Mesoproterozoic crustal materials. The results of isotopic compositions of the Dak Krong plutonic rocks are slightly lower than those of

the Hai Van and Van Canh granites (Hieu et al., 2015; Hung et al., 2019).

Zircon saturation temperature calculated for granites in Dak Krong at ranges of 719-797°C and 657-754°C applying the estimations of Watson and Harrison (1983) and Boehnke et al. (2013), respectively, may be indicative of "cold" granites, referred to as inheritance-rich (ca. 766°C) rather than "hot" and inheritance-poor (ca. 837°C) granites (Miller et al., 2003). Additionally, xenocrystic zircon sporadically observed in the zircons cores of the Dak Krong granites might be considered a sign of "cold" granites. Accordingly, with the disseminated inherited zircon, it is presumable that the contribution of the heat from the mantle is negligible. The input heat and material sources contributing to Permian-Triassic magmatism have been thoroughly discussed by Faure et al. (2018). Accordingly, although the Emeishan plume does not seem to provide input materials for the magmas in the study area and its vicinities, the heat might have been produced and transferred from the mantle plume to the lithosphere of the Indochina Block. The heat flow might have been facilitated and modified by the Permian-Triassic geodynamics of the post-collisional slab break-off.

5.3. Tectonic settings generating Permian-Triassic plutonism in Dak Krong and the adjacent areas

Permian-Triassic magmatism along the NW-SE-trending Song Ma Suture Zone, the Truong Son Belt, and the Kontum Massif have widely been correlated to the subduction and disappearance of Paleo-Tethys (Carter et al., 2001; Hoa et al., 2008; Hung et al., 2022; Pham et al., 2022; Shi et al., 2015; Thanh et al., 2019; Tran et al., 2014; Wang et al., 2016). Although far-field influenced by the closure of Paleo-Tethys and Indochina-South China amalgamation, they have been proven to link to this event. Considering the continuity of the geographical distribution of the Dak Krong granites to the surrounding coeval plutonic, they can presumably relate to this event.

Figure 11 shows the emplacements of numerous Permian-Triassic granitoid bodies throughout Vietnam's northern to central parts. They have been systemized according to the tectonic environments from which they were generated: intra-continental rift and subduction. Also shown in Figure 11 is the structural framework from north to south with a common NW-SE orientation and I- or S-type granitoid bodies with the dominance of I-type granitoids over the S-type and other undefined granitoids with ambiguous affinities. Several tectonic environments have been assigned to account for the various rock types, such as the Emeishan mantle plume event (ca. 262-245 Ma) generating A-type granites and associated volcanics (Hieu et al., 2013; Minh et al., 2018; Pham et al., 2022; Tran et al., 2015; Shellnutt et al., 2020), Paleo-Tethys subduction generating mainly I-type granites and the collisional setting accounting for S-type granites (Carter et al., 2001; Hieu et al., 2017, 2020; Shi et al., 2015; Wang et al., 2016). According to obtained data in this study, it is suggested that the Dak Krong granites and other Permian-Triassic rocks in the Kontum Massif are generated by subduction-related and consequential collisional regimes (Fig. 11).

Another evidence for this correlation is that the chemical compositions of the Dak Krong granites are similar to Permian-Triassic arc-related magmas with almost identical chemical composition with plutonic rocks in previous studies (e.g., Ben Giang-Que Son, Hai Van usually ascribed to syn- to post-collision magmatism and Van Canh rocks). This observation proves they might have been fractionated from the same or close magma chamber regarding genetic relationship but different in fractionation degrees.

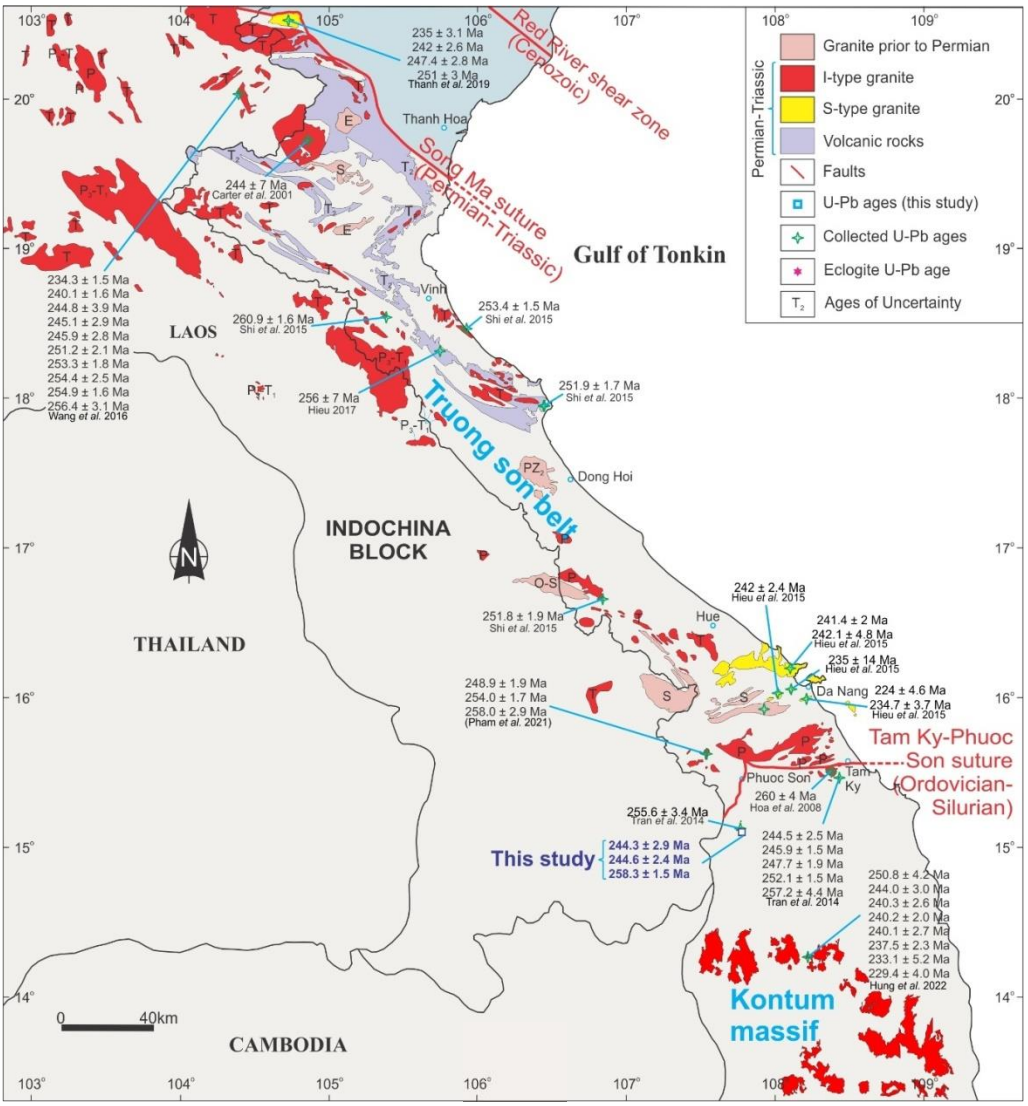

Figure 11. Schematic map showing the tectonic structures and spatial distribution of granitoid bodies throughout northern and central Vietnam; age data compiled from (Carter et al., 2001; Hieu et al., 2015, 2017, 2020; Hoa et al., 2008; Hung et al., 2022; Pham et al., 2022; Shi et al., 2015; Thanh et al., 2019; Tran et al., 2014; Wang et al., 2016)

The Po Ko River, commonly referred to as the Po Ko Suture Zone, and the Tam Ky-Phuoc Son suture zone, has been suggested to mark the closure of an Early Paleozoic ancient ocean basin (Tran et al., 2014). It should be noted in this study that these suture zones are not genetically related to the Dak Krong granites and other Permian-Triassic magmas in the Kontum Massif. However, the collected samples are located along the Po Ko River. Instead, the two stages of magmatism (ca. 258 Ma and 245 Ma) in this study are likely related to the Paleo-Tethys subduction and syn-collision between the South China and Indochina Blocks (Fig. 12). Alternatively, the Emeishan mantle plume event that mainly gave rise to the Permian-Triassic magmas in the Phan Si Pan zone and Tu Le basin has

been proposed to generate magmatic activity in the Kontum Massif (e.g., Faure et al., 2018; Owada et al., 2016). However, magmas related to this event are characterized by a cluster of A-type granites, occurring among ultramafic-mafic rocks of the Song Da intraplate rift, with positive $\varepsilon_{Hf}(t)$ values, low- to high-Ti signatures (Hieu et al., 2013; Usuki et al., 2015; Minh et al., 2018; Pham et al., 2022) and are not commonly observed in Permian-Triassic granitoids in the Kontum Massif. Therefore, the hypothesis of the closure of a Paleo-Tethys branch and the following syn-collision between the South China and Indochina Blocks seems to be more likely.

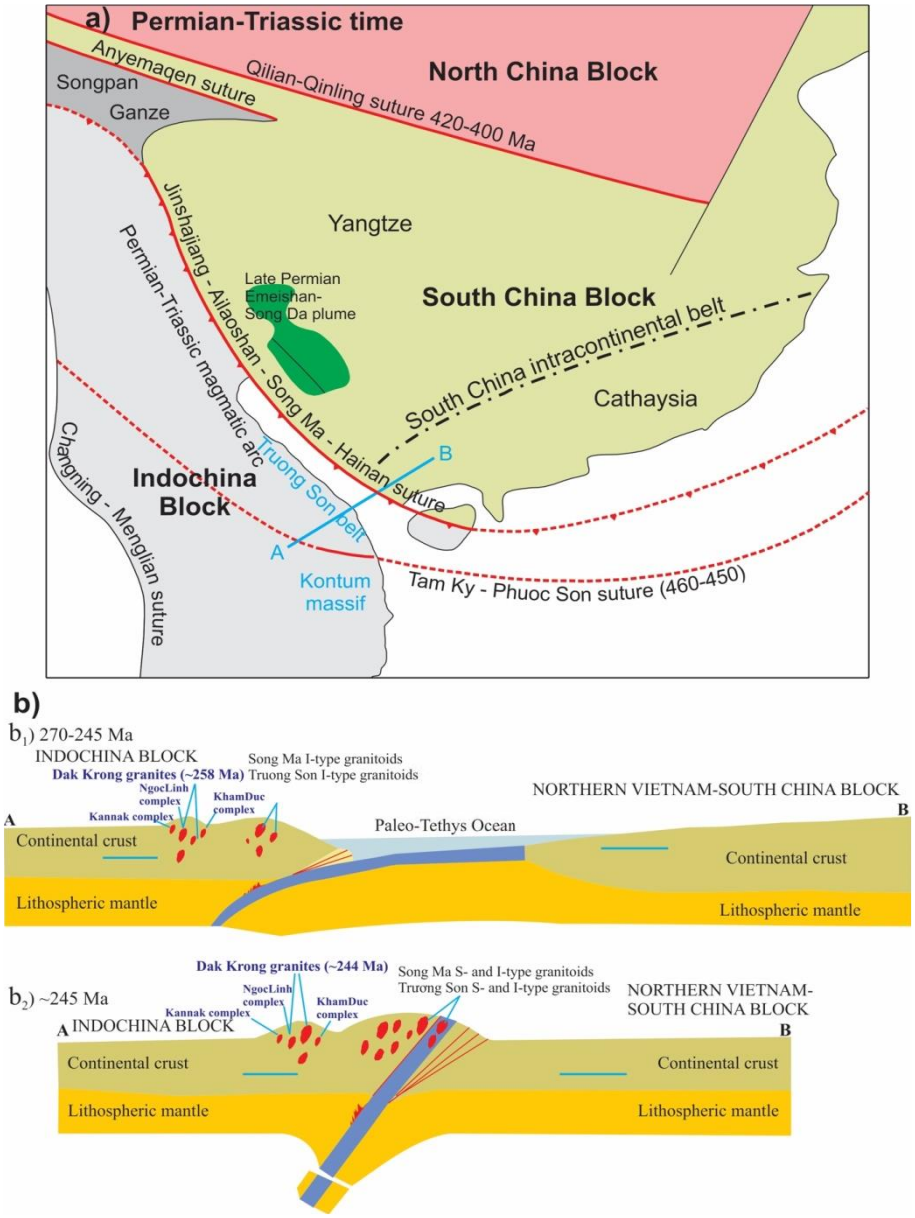

Figure 12. Tectonic setting generating Dak Krong magmas in the Kontum Massif and adjacent areas (Faure et al., 2018; Hieu et al., 2020)

6. Conclusions

The Dak Krong plutonic rocks in the Kontum Massif show a narrow range of petrographical compositions, mainly pointing to granite field with a major mineral assemblage of plagioclase, hornblende, quartz, biotite, and K-feldspar. Metaluminous and high-K affinities characterize them and presumably originated from a collisional regime, most likely the early stage of syn-collision.

The Hf isotope data from zircon with εHf(t) ranging between -6.4 and -0.5 indicates a crustal signature. With zircon Hf model ages (TDM2) ranging from 1165-1497 Ma, it is suggested that the Dak Krong plutonic rocks are the product of partial melting of Mesoproterozoic crustal materials with a negligible contribution of mantle materials.

Zircon U-Pb age dating results show two main age clusters: 258 Ma and 245 Ma temporally corresponding to the subduction and syn-collisional stages of Paleo-Tethys evolution extensively recorded along the Song Ma Suture Zone and Truong Son Belt regarded as Indosinian Orogeny.

Acknowledgments

This research was funded by Vietnam National University Ho Chi Minh City (VNU-HCM) under grant number B2019-18-08/HĐ-KHCN. Thanks to Prof. Wang W, China University of Geosciences, for helping with the sample analysis. The manuscript benefits from constructive comments and suggestions of the editorial board, Prof. Michel Faure, and an anonymous reviewer that are gratefully acknowledged.

References

Bao N.X., 2000. Tectonics and metallogeny of southern Vietnam, Project Report. South Vietnam Geological Mapping Division (in Vietnamese), Hochiminh.

Boehnke P., Watson E.B., Trail D., Harrison T.M., Schmitt A.K., 2013. Zircon saturation re-revisited. Chemical Geology, 351, 324-334.

Bouvier A., Vervoort J.D., Patchett P.J., 2008. The Lu-Hf and Sm-Nd isotopic composition of CHUR: Constraints from unequilibrated chondrites and implications for the bulk composition of terrestrial planets. Earth and Planetary Science Letters, 273, 48-57.

Bui M.T., Le D.B., Nguyen D.T., Nguyen H.T., Nguyen L.N., Pham D.L., Tran T.H., Tran T.A., Trinh V.L., Trinh X.H., 2010. Magmatism in Vietnam. Mapping Publishing House, Hanoi.

Carter A., Roques D., Bristow C., Kinny P., 2001. Understanding Mesozoic accretion in Southeast Asia: significance of Triassic thermotectonism (Indosinian orogeny) in Vietnam. Geology, 29, 211-214.

Chappell B.W., Bryant C.J., Wyborn D., White A.J.R., Williams, I.S., 1998. High-and low temperature I type granites. Resource Geology, 48, 225-235.

Chappell B.W., White A.J.R., Williams I.S., Wyborn D., 2004. Low-and high-temperature granites, in: Special Paper of the Geological Society of America. Geological Society of America, 125-140.

Cox K.G., Bell J.D., Pankhurst R.J., 1979. The interpretation of igneous rocks. London, Allen.

Faure M., Lepvrier C., Nguyen V. Van, Vu T. Van, Lin W., Chen Z., 2014. The South China block-Indochina collision: Where, when, and how? Journal of Asian Earth Sciences, 79, 260-274.

Faure M., Nguyen V.V., Hoai L.T.T., Lepvrier C., 2018. Early Paleozoic or Early-Middle Triassic collision between the South China and Indochina Blocks: The controversy resolved? Structural insights from the Kon Tum massif (Central Vietnam). Journal of Asian Earth Sciences, 166, 162-180.

Griffin W.L., Pearson N.J., Belousova E., Jackson S.E., van Achterbergh E., O'Reilly S.Y., Shee S.R., 2000. The Hf isotope composition of cratonic mantle: LAM-MC-ICPMS analysis of zircon megacrysts in kimberlites. Geochimica et Cosmochimica Acta, 64, 133-147.

Harris N.B.W., Pearce J.A., Tindle A.G., 1986. Geochemical characteristics of collision-zone magmatism. Geological Society, London, Special Publications, 19, 67-81.

Hieu P.T., Anh N.T., Minh P., Thuy N.T., 2020. Geochemistry, zircon U-PB ages and HF isotopes of the Muong Luan granitoid pluton, Northwest Vietnam and its petrogenetic significance. Island Arc., 29(1), e12330.

Hieu P.T., Chen F.K., Thuy N.T.B., Quoc Cuong N., Li S.Q., 2013. Geochemistry and zircon U-Pb ages and Hf isotopic composition of Permian alkali granitoids of the Phan Si Pan zone in northwestern Vietnam. Journal of Geodynamics, 69, 106-121.

Hieu P.T., Li S.Q., Yu Y., Thanh N.X., Dung L.T., Tu V. Le, Siebel W., Chen F., 2017. Stages of late Paleozoic to early Mesozoic magmatism in the Song Ma belt, NW Vietnam: evidence from zircon U-Pb geochronology and Hf isotope composition. International Journal of Earth Sciences, 106, 855-874.

Hieu P.T., Yang Y.-Z., Binh D.Q., Nguyen T.B.T., Dung L.T., Chen F., 2015. Late Permian to Early Triassic crustal evolution of the Kontum massif, central Vietnam: zircon U-Pb ages and geochemical and Nd-Hf isotopic composition of the Hai Van granitoid complex. International Geology Review, 57, 1877-1888.

Hoa T.T., Anh T.T., Phuong N.T., Dung P.T., Anh T.V., Izokh A.E., Borisenko A.S., Lan C.Y., Chung S.L., Lo C.H., 2008. Permo-Triassic intermediate-felsic magmatism of the Truong Son belt, eastern margin of Indochina. Comptes Rendus Geoscience, 340, 112-126.

Hoskin P.W.O., Schaltegger U., 2003. The Composition of Zircon and Igneous and Metamorphic Petrogenesis. Reviews in Mineralogy and Geochemistry, 53, 27-62.

Hung D.D., Tsutsumi Y., Hieu P.T., Minh N.T., Minh P., Dung N.T., Hung N.B., Komatsu T., Hoang N., Kawaguchi K., 2022. Van Canh Triassic granite in the Kontum Massif, central Vietnam: geochemistry, geochronology, and tectonic implications. Journal of Asian Earth Sciences, X(7), 100075.

Khuc V., 2000. The Triassic of Indochina Peninsula and its interregional correlation. In Developments in Palaeontology and Stratigraphy. Elsevier, 18, 221-233.

Lepvrier C., Maluski H., Van Tich V., Leyreloup A., Truong Thi P., Van Vuong N., 2004. The Early Triassic Indosinian orogeny in Vietnam (Truong Son Belt and Kontum Massif); implications for the geodynamic evolution of Indochina. Tectonophysics, 393, 87-118.

Lepvrier C., Van Vuong N., Maluski H., Truong Thi P., Van Vu T., 2008. Indosinian tectonics in Vietnam. Comptes Rendus-Geoscience, 340, 94-111.

Liu J., Tran M.-D., Tang Y., Nguyen Q.-L., Tran T.-H., Wu W., Chen J., Zhang Z., Zhao Z., 2012. Permo-Triassic granitoids in the northern part of the Truong Son belt, NW Vietnam: Geochronology, geochemistry and tectonic implications. Gondwana Research, 22, 628-644.

Ludwig K.R., 2008. Isoplot 3.6. Berkeley Geochronology Center Special Publication, 4, 77.

Metcalfe I., 2013. Gondwana dispersion and Asian accretion: Tectonic and palaeogeographic evolution of eastern Tethys. Journal of Asian Earth Sciences, 66, 1-33.

Metcalfe I., 2017. Tectonic evolution of Sundaland. Bulletin of the Geological Society of Malaysia, 63, 27-60.

Miller C.F., McDowell S.M., Mapes R.W., 2003. Hot and cold granites: Implications of zircon saturation temperatures and preservation of inheritance. Geology, 31, 529-532.

Minh P., Hieu P.T., Hoang N.K., 2018. Geochemical and geochronological studies of the Muong Hum alkaline granitic pluton from the Phan Si Pan Zone, northwest Vietnam: Implications for petrogenesis and tectonic setting. Island Arc., 27, e12250.

Nakano N., Osanai Y., Owada M., Nam T.N., Charusiri P., Khamphavong K., 2013. Tectonic evolution of high-grade metamorphic terranes in central Vietnam: Constraints from large-scale monazite geochronology. Journal of Asian Earth Sciences, 73, 520-539.

Nguyen T.T.B., Satir M., Siebel W., Chen F., 2004. Granitoids in the Dalat zone, southern Vietnam: age constraints on magmatism and regional geological implications. International Journal of Earth Sciences, 93, 329-340.

Owada M., Osanai Y., Nakano N., Adachi T., Kitano I., Van Tri T., Kagami H., 2016. Late Permian plume-related magmatism and tectonothermal events in the Kontum Massif, central Vietnam. Journal of Mineralogical and Petrological Sciences, 111, 181-195.

Pearce J.A., Harris N.B.W., Tindle A.G., 1984. Trace element discrimination diagrams for the tectonic interpretation of granitic rocks. Journal of Petrology, 25, 956-983.

Peccerillo A., Taylor S.R., 1976. Geochemistry of Eocene calc-alkaline volcanic rocks from the Kastamonu area, northern Turkey. Contributions to Mineralogy and Petrology, 58, 63-81.

Pham M., Pham Trung H., Kawaguchi K., Nong Thi Quynh A., Le Duc P., 2022. Geochemistry, zircon

U-Pb geochronology and Sr-Nd-Hf isotopic composition of the Cha Val plutonic rocks in central Vietnam: Implications for Permian-Triassic Paleo-Tethys subduction-related magmatism. Vietnam J. Earth Sci., 44(3), 301-326. https://doi.org/10.15625/2615-9783/16842.

Pham T.T., Shellnutt J.G., Tran T.A., Denyszyn S.W., Iizuka Y., 2022. Petrogenesis of silicic rocks from the Phan Si Pan-Tu Le region of the Emeishan large igneous province, northwestern Vietnam. Geological Society, London, Special Publications, 518, 227-254.

Sang D.Q., 2011. Petrographic characteristics and zircon U-Pb geochronology of granitoid rocks in the southern Ben Giang, Quang Nam province. Science and Technology Development Journal, 14, 17-30.

Scherer E., Münker C., Mezger K., 2001. Calibration of the Lutetium-Hafnium Clock. Science, 293, 683-687.

Shand S.J., 1943. The eruptive rocks, 2nd ed. John Wiley, New York.

Shellnutt J.G., Lan C.Y., Van Long T., Usuki T., Yang H.J., Mertzman S.A., Iizuka Y., Chung S.L., Wang K.L., Hsu W.Y., 2013. Formation of Cretaceous Cordilleran and post-orogenic granites and their microgranular enclaves from the Dalat zone, southern Vietnam: Tectonic implications for the evolution of Southeast Asia. Lithos, 182-183, 229-241.

Shellnutt J.G., Pham T.T., Denyszyn S.W., Yeh M.W., Tran T.A., 2020. Magmatic duration of the Emeishan large igneous province: Insight from northern Vietnam. Geology, 48, 457-461.

Shi M.F., Lin F.C., Fan W.Y., Deng Q., Cong F., Tran M.D., Zhu H.P., Wang H., 2015. Zircon U-Pb ages and geochemistry of granitoids in the Truong Son terrane, Vietnam: Tectonic and metallogenic implications. Journal of Asian Earth Sciences, 101, 101-120.

Sun S.S., McDonough W.F., 1989. Chemical and isotopic systematics of oceanic basalts: Implications for mantle composition and processes. Geological Society Special Publication, 42, 313-345.

Thanh N.X, Tu M.T., Itaya T., Kwon S., 2011. Chromian-spinel compositions from the Bo Xinh ultramafics, Northern Vietnam: Implications on tectonic evolution of the Indochina block. Journal of Asian Earth Sciences, 42, 258-267.

Thanh T. V., Hieu P.T., Minh P., Nhuan D. Van, Thuy N.T.B., 2019. Late Permian-Triassic granitic rocks of Vietnam: the Muong Lat example. International Geology Review, 61, 1823-1841.

Thuy N.T.B., Satir M., Siebel W., Vennemann T., Long T. Van, 2004. Geochemical and isotopic constraints on the petrogenesis of granitoids from the Dalat zone, southern Vietnam. Journal of Asian Earth Sciences, 23, 467-482.

Tran H.T., Zaw K., Halpin J.A., Manaka T., Meffre S., Lai C.K., Lee Y., Le H. Van, Dinh S., 2014. The Tam Ky-Phuoc Son Shear Zone in central Vietnam: Tectonic and metallogenic implications. Gondwana Research, 26, 144-164.

Tran T.H., Lan C.Y., Usuki T., Shellnutt J.G., Pham T.D., Tran T.A., Pham N.C., Ngo T.P., Izokh A.E., Borisenko A.S., 2015. Petrogenesis of Late Permian silicic rocks of Tu Le basin and Phan Si Pan uplift (NW Vietnam) and their association with the Emeishan large igneous province. Journal of Asian Earth Sciences, 109, 1-19.

Trang N.V., 1986. Geology and Mineral Resources Map of Vietnam scale 1:200,000, Hue-Quang Ngai sheet series. Department of Geology and Minerals of Vietnam, Hanoi.

Tri T.V., Khuc V., 2009. Geology and natural resources of Vietnam. Natural Science and Technology Publishing House, Hanoi, 589p.

Usuki T., Lan C.Y., Yui T.F., Iizuka Y., Van Vu T., Tran T.A., Okamoto K., Wooden J.L., Liou J.G., 2009. Early Paleozoic medium-pressure metamorphism in central Vietnam: evidence from SHRIMP U-Pb zircon ages. Geosciences Journal, 13(3), 245-256.

Wang S., Mo Y., Wang C., Ye P., 2016. Paleotethyan evolution of the Indochina Block as deduced from granites in northern Laos. Gondwana Research, 38, 183-196.

Watson E.B., Harrison T.M., 1983. Zircon saturation revisited: temperature and composition effects in a variety of crustal magma types. Earth and Planetary Science Letters, 64, 295-304.

Whalen J.B., Currie K.L., Chappell B.W., 1987. A-type granites: geochemical characteristics, discrimination and petrogenesis. Contributions to Mineralogy and Petrology, 95, 407-419.